

Asymptotic model for shape resonance control of diatomics by intense non-resonant light:
universality in the single-channel approximation

This content has been downloaded from IOPscience. Please scroll down to see the full text.

2015 New J. Phys. 17 045022

(<http://iopscience.iop.org/1367-2630/17/4/045022>)

View [the table of contents for this issue](#), or go to the [journal homepage](#) for more

Download details:

IP Address: 141.51.198.148

This content was downloaded on 28/04/2015 at 10:23

Please note that [terms and conditions apply](#).



PAPER

Asymptotic model for shape resonance control of diatomics by intense non-resonant light: universality in the single-channel approximation

OPEN ACCESS

RECEIVED

23 December 2014

REVISED

18 March 2015

ACCEPTED FOR PUBLICATION

24 March 2015

PUBLISHED

27 April 2015

Content from this work
may be used under the
terms of the [Creative
Commons Attribution 3.0
licence](#).

Any further distribution of
this work must maintain
attribution to the
author(s) and the title of
the work, journal citation
and DOI.

Anne Crubellier^{1,5}, Rosario González-Férez^{2,3}, Christiane P Koch⁴ and Eliane Luc-Koenig¹¹ Laboratoire Aimé Cotton, CNRS, Université Paris-Sud 11, ENS Cachan, Bâtiment 505, F-91405 Orsay Cedex, France² Instituto Carlos I de Física Teórica y Computacional and Departamento de Física Atómica, Molecular y Nuclear, Universidad de Granada, E-18071 Granada, Spain³ The Hamburg Center for Ultrafast Imaging, University of Hamburg, Luruper Chaussee 149, D-22761 Hamburg, Germany⁴ Theoretische Physik, Universität Kassel, Heinrich-Plett-Str. 40, D-34132 Kassel, Germany⁵ Author to whom any correspondence should be addressed.E-mail: anne.crubellier@u-psud.fr, rogonzal@ugr.es, christiane.koch@uni-kassel.de and eliane.luc@u-psud.fr

Keywords: cold molecules, shape resonances, universality

Abstract

Non-resonant light interacting with diatomics via the polarizability anisotropy couples different rotational states and may lead to strong hybridization of the motion. The modification of shape resonances and low-energy scattering states due to this interaction can be fully captured by an asymptotic model, based on the long-range properties of the scattering (Crubellier *et al* 2015 *New J. Phys.* **17** 045020). Remarkably, the properties of the field-dressed shape resonances in this asymptotic multi-channel description are found to be approximately linear in the field intensity up to fairly large intensity. This suggests a perturbative single-channel approach to be sufficient to study the control of such resonances by the non-resonant field. The multi-channel results furthermore indicate the dependence on field intensity to present, at least approximately, universal characteristics. Here we combine the nodal line technique to solve the asymptotic Schrödinger equation with perturbation theory. Comparing our single channel results to those obtained with the full interaction potential, we find nodal lines depending only on the field-free scattering length of the diatom to yield an approximate but universal description of the field-dressed molecule, confirming universal behavior.

1. Introduction

Quantum collisions at low energy depend on the long-range properties of the interaction between the particles only and therefore exhibit universal behavior. Since, at long range, the dependence of the interaction on interparticle distance has a power-law form and it is often sufficient to account only for the highest order term of the interaction, low-energy collisions can be well described by simple models with very few free parameters. This is at the core of multi-channel quantum defect theory [1–8]. Universality becomes particularly transparent when introducing units which absorb all molecule-specific parameters [9]. The corresponding Schrödinger equation can be solved by the so-called nodal line technique [10–12]. It consists in accounting for all short-range physics by the choice of the node positions of the scattering wavefunction at intermediate interparticle distances. This formalism has been extended to shape resonances [13] and to the control of shape resonances by non-resonant light which couples the different partial ℓ -waves via the polarizability anisotropy [14]. In particular, we have previously shown that an intensity-dependent nodal line is sufficient to account for the effect of the coupling to the non-resonant light at short-range. An asymptotic multi-channel model can thus predict the resonance structure, energy, width and hybridization as a function of non-resonant light intensity. This is important since non-resonant light control has been suggested to enhance photoassociation rates [15, 16], modify Feshbach resonances [17] and manipulate molecular levels [16, 18].

While a multi-channel treatment is essential to describe the strong hybridization of the rovibrational motion due to the coupling with the non-resonant light [15, 16], the position and width of the resonance are found to vary linearly with field intensity up to fairly large intensities [14]. When treating the interaction with the non-resonant light as a perturbation and truncating the perturbation expansion at the first order, resonance position and width are determined by the field-free wavefunctions. The field-free wavefunctions reside in a single partial wave (channel) and, within the asymptotic approximation, depend on only one parameter—the *s*-wave scattering length. This indicates universality of the intensity dependence of resonance positions and widths in non-resonant light control. It furthermore suggests that a single-channel approach should be sufficient to study non-resonant light control at moderate intensities.

Here we combine the asymptotic model for shape resonance control with non-resonant light developed in a preceding paper [14] with perturbation theory to explore the universality of the resonance's intensity dependence. This allows us to recast the multi-channel approach of [14] in a single channel approximation. We compare the perturbative results to those obtained in [14] with a multi-channel description, by solving the Schrödinger equation for the diatom interacting with non-resonant light both with the full potential and the asymptotic approximation.

The paper is organized as follows: we briefly review the asymptotic model for a diatomic interacting with non-resonant light via the polarizability anisotropy introduced in [14], hereafter referred to as paper I, in section 2. We summarize the behavior of shape resonances in non-resonant light observed by solving the multi-channel Schrödinger equation and present an approximate general law for describing the intensity dependence when analyzing the resonances in reduced units of length and energy in section 3. We then show in section 4 how perturbation theory, either using energy-normalized continuum states (section 4.1) or a discretized continuum (section 4.2), is applied to determine the slopes of the intensity dependence of position and width of the field-dressed shape resonances at vanishing intensity. This allows us to explain the rule observed for the specific example of strontium dimers considered in paper I. Then, section 5.1 describes systematic single-channel calculations that allow for predicting the position and width of shape resonances without a non-resonant field. These results are used in section 5.2 to deduce the slope of the energy shifts of a shape resonance in the limit of vanishing intensity for any angular momentum ℓ , in any diatomic system. We conclude in section 6.

2. Asymptotic model for a diatom in a non-resonant optical field

In this section, we summarize the theoretical framework for studying the interaction of a diatom with non-resonant light. A detailed derivation of the asymptotic model is found in [14]. The rovibrational Hamiltonian of an atom pair, with reduced mass μ , interacting with a non-resonant laser field of intensity I , linearly polarized along the space-fixed Z axis, is written in the molecule-fixed frame as [18]

$$H = T_R + \frac{\mathbf{L}^2}{2\mu R^2} + V_g(R) - \frac{2\pi I}{c} \left(\Delta\alpha(R) \cos^2\theta + \alpha_{\perp}(R) \right). \quad (1)$$

Here, R denotes interatomic separation and $V_g(R)$ the interaction potential in the electronic ground state. T_R and $\mathbf{L}^2/2\mu R^2$ are the vibrational and rotational kinetic energies. In the last term of equation (1), c is the speed of light and θ the polar angle between the molecular axis and the laser polarization. The molecular polarizability tensor is characterized by its perpendicular and parallel components with respect to the molecular axis $\alpha_{\perp}(R)$ and $\alpha_{\parallel}(R)$, and the polarizability anisotropy is $\Delta\alpha(R) = \alpha_{\parallel}(R) - \alpha_{\perp}(R)$. Hamiltonian (1) is valid for any diatomic molecule in its electronic ground state [18, 19]. The non-resonant field introduces a mixing of different partial waves ℓ of the same parity (channels), whereas the magnetic quantum number m is conserved. For the sake of simplicity, this study is restricted to states with $m = 0$ for which the largest effect of the non-resonant field is observed. The corresponding multi-channel Schrödinger equation can be solved numerically, for $m = 0$, as described in [16].

At sufficiently large distance, $R > R_{\text{asym}} = \sqrt{C_8/C_6}$, the potential reduces to the asymptotic van der Waals interaction $V_g(R) \approx -C_6/R^6$ (C_n are the coefficients of the multipolar expansion). For $R \gg R_d = (4\alpha_1\alpha_2)^{1/6}$, where α_1, α_2 denote the polarizabilities of the two atoms, the interaction with the field reduces to

$$H_{\text{int}} = -\frac{2\pi I}{c} \left[(\alpha_1 + \alpha_2) + \frac{2\alpha_1\alpha_2}{R^3} (3 \cos^2\theta - 1) \right]. \quad (2)$$

Introducing a dimensionless reduced length x , $R = \sigma x$, a reduced energy \mathcal{E} , $E - E_0 = \epsilon \mathcal{E}$ (defined with respect to the field shifted dissociation limit $E_0 = -\frac{2\pi}{c}(\alpha_1 + \alpha_2)I$), and a reduced laser field intensity \mathcal{I} , $I = \beta \mathcal{I}$, and replacing all R -dependent terms by their leading order contributions, an asymptotic Schrödinger equation is obtained,

Table 1. Scaling factors, equations (4), for $^{88}\text{Sr}_2$ and $^{86}\text{Sr}^{88}\text{Sr}$, obtained for $C_6 = 3246.97$ a.u. and $\alpha_0 = 186.25$ a_0^3 , and for $^{133}\text{Cs}_2$ ($C_6 = 6851.0$ a.u., $\alpha_0 = 402.20$ a_0^3) and $^{87}\text{Rb}_2$ ($C_6 = 4707.0$ a.u., $\alpha_0 = 309.98$ a_0^3); a.u. denotes the atomic units and a_0 the Bohr radius.

	σ (a_0)	ϵ (μK)	β (GW cm^{-2})	τ (ns)
$^{88}\text{Sr}_2$	151.053	86.3653	0.635 782	88.4409
$^{86}\text{Sr}^{88}\text{Sr}$	150.617	87.876	0.641 319	86.9204
$^{133}\text{Cs}_2$	201.843	31.99	0.120 48	238.7
$^{87}\text{Rb}_2$	165.250	72.99	0.258 44	104.5

Table 2. Characteristic internuclear distances for $^{88}\text{Sr}_2$ interacting with non-resonant light in atomic units (R , first line) and reduced units (x , second line), see equations (4) and table 1 for the definition of the reduced units. R_w denotes the position of the repulsive wall of V_g , R_e its equilibrium distance. The validity of the asymptotic model with respect to the interaction with the non-resonant field is characterized by $R_d = (4\alpha_1\alpha_2)^{1/6}$ and $R_C > R_d$ [14] and by $R_{\text{asym}} = \sqrt{C_8/C_6}$ concerning V_g . $R_{0\ell}$, R_b and R_{top} indicate (for $\ell = 2 \dots 20$) the range of the node position, cf equation (6), the inner limit and the top of the rotational barrier, respectively (see figure 4 in [13]).

	R_w	R_e	R_d	R_C	R_{asym}	$R_{0\ell}$	R_b	R_{top}
a.u.	7.5	8.5	7.3	10	11	24...26	97...33	127...44
red.u.	0.050	0.056	0.048	0.066	0.073	0.16...0.17	0.64...0.22	0.84...0.29

$$\left[-\frac{d^2}{dx^2} - \frac{1}{x^6} + \frac{L^2}{x^2} - \mathcal{I} \frac{\cos^2 \theta - 1/3}{x^3} - \mathcal{E} \right] f(x, \theta, \varphi) = 0. \quad (3)$$

where φ denotes the azimuthal angle around the molecular axis. The unit conversion factors are given by

$$\sigma = \left(\frac{2\mu C_6}{\hbar^2} \right)^{1/4}, \quad \epsilon = \frac{\hbar^2}{2\mu\sigma^2}, \quad \beta = \frac{c\sigma^3\epsilon}{12\pi\alpha_1\alpha_2}, \quad (4)$$

and the conversion factor for time is obtained from that for energy, $\tau = \hbar/\epsilon$. The corresponding conversion factors are collected in table 1 for some example diatomics.

For each partial wave ℓ , the wave function is expanded in terms of spherical harmonics $Y_{\ell,m=0}(\theta, \varphi)$

$$f_{\ell}(x, \theta, \varphi) = y_{\ell}(x) Y_{\ell,m=0}(\theta, \varphi), \quad (5)$$

and equation (3) is solved in the asymptotic x -domain, imposing to the radial function physical boundary condition at long range and a node at $x_{0\ell} > x_{\text{asym}} = R_{\text{asym}}/\sigma > x_d = R_d/\sigma$, a position separating inner zone and asymptotic outer region, see [14] for details. Table 2 lists the values of R_{asym} , R_d and other characteristic internuclear distances for the example of $^{88}\text{Sr}_2$. The effects of potential $V_g(R)$, centrifugal energy and polarizability in the inner zone can satisfactorily be accounted for by introducing energy-, angular-momentum- and intensity-dependent nodal lines $x_{0\ell}$ [13, 14],

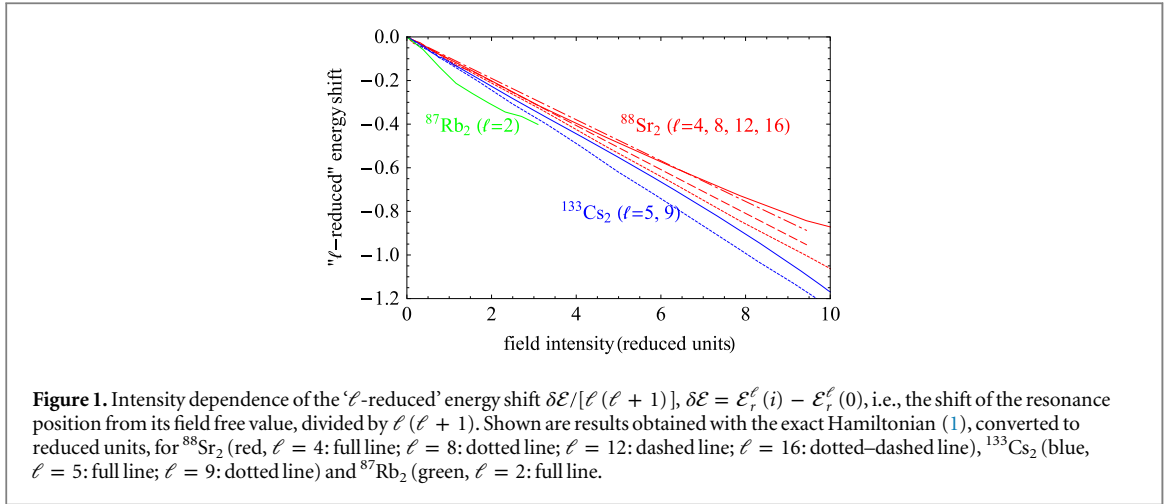
$$x_{0\ell} = x_{00} + A e + B\ell(\ell + 1) + C\mathcal{I}. \quad (6)$$

When the constants A , B and C can be deduced from exact calculations using the Hamiltonian (1) or from experiment, the nodal line technique applied to the asymptotic model fully reproduces the results obtained with (1), cf figure 2 of [14]. When this is not possible, analytical values for A^G , B^G [13] and C^G [14] which depend on x_{00} , i.e., on the s -wave scattering length, allow for an approximate, universal description of shape resonances, very similar to the asymptotic model developed by Gao for field-free resonances [20].

3. Heuristic scaling rule

We present and discuss in this section results obtained by solving the Schrödinger equation with the exact Hamiltonian (1), using the discrete variable representation (DVR) as described in [16]. Specifically, we consider the shape resonances with field-free $\ell = 4, 8, 12, 16$ for $^{88}\text{Sr}_2$ [16], $\ell = 5, 9$ for $^{133}\text{Cs}_2$, and $\ell = 2$ for $^{87}\text{Rb}_2$. In paper I [14], a linear dependence of the resonance position versus field intensity was found for the two considered isotopes $^{88}\text{Sr}_2$ and $^{86}\text{Sr}^{88}\text{Sr}$ up to very large values of the intensity [14]. The use of reduced units (see table 1) allows us to extract from these results a general trend for the intensity dependence of the resonance position, valid also for different ℓ values and different species.

To this end, we introduce ‘ ℓ -reduced’ energy shifts or slopes. These are the energy shifts or slopes, in reduced units, divided by $\ell(\ell + 1)$. More precisely, for a field-dressed shape resonance adiabatically correlated to a field-free resonance in the partial wave ℓ , which occurs at the reduced energy $\mathcal{E}_r^{\ell}(\mathcal{I})$ for a non-resonant field of



reduced intensity \mathcal{I} , the ‘ ℓ -reduced’ energy shift is equal to $\delta\mathcal{E}/[\ell(\ell+1)]$, where $\delta\mathcal{E} = \mathcal{E}_r^\ell(\mathcal{I}) - \mathcal{E}_r^\ell(0)$ denotes the shift of the resonance from its field-free position (here, as everywhere else in the paper, the position of a shape resonance is taken with respect to the field shifted dissociation limit). Analogously, we call the quantity $\delta\mathcal{E}/[\mathcal{I}\ell(\ell+1)]$ ‘ ℓ -reduced’ slope. The intensity dependence of the ‘ ℓ -reduced’ energy shifts is reported in figure 1 for the resonances in strontium, rubidium and cesium mentioned above. Except for the $\ell = 2$ resonance in $^{87}\text{Rb}_2$, an almost linear behavior is observed up to high intensity. Moreover, in the limit of vanishing field all slopes are nearly equal.

Before presenting a calculation of the slopes to first order of perturbation in section 4, we give here a simple qualitative argument, based on perturbation theory, to justify the approximate proportionality to $\ell(\ell+1)$ of the slope of the resonance position’s intensity-dependence at vanishing intensity. The asymptotic interaction with the field, given in reduced units by

$$h_{\text{int}} = -\mathcal{I}/x^3 \left(\cos^2 \theta - 1/3 \right), \quad (7)$$

can be treated as a perturbation and therefore, to first order, in a single-channel approach. One has thus to calculate the matrix element of h_{int} with the (single-channel) field-free wave functions $f_\ell^{I=0}(x, \theta, \varphi)$ (see equation (A.7) in appendix),

$$\begin{aligned} & \left\langle f_\ell^{I=0}(x, \theta, \varphi) \left| h_{\text{int}} \right| f_\ell^{I=0}(x, \theta, \varphi) \right\rangle \\ &= -\mathcal{I} \alpha(\ell) \int_{x_{0\ell}}^{\infty} \left[y_\ell^{I=0} \right]^2 x^{-3} dx \end{aligned} \quad (8)$$

with $m = 0$ and

$$\alpha(\ell) = \frac{2\ell(\ell+1)}{3(2\ell+3)(2\ell-1)}. \quad (9)$$

An integral similar to the one in equation (8) occurs in the expectation value of R^{-3} for field-free wave functions obtained with the exact Hamiltonian (1), when $x_{0\ell}$ is replaced by $R = 0$. It is important to note that, for $\ell \geq 2$, the angular factor $\alpha(\ell)$ is nearly independent of ℓ and approximately equal to $1/6$. The ℓ -dependence of the matrix element, equation (8), thus necessary arises from the radial part, i.e., the expectation value of x^{-3} for the field free wave functions.

The field-free resonance positions result from the competition between the van der Waals and centrifugal interactions at intermediate distance, where the amplitude of the resonance wave function is very large. Intermediate distances are already in the asymptotic zone, but well before the location x_ℓ of the potential barrier, i.e., $x_{\text{asym}} < x_{0\ell} < x \ll x_\ell$. Here $x_{\text{asym}} = R_{\text{asym}}/\sigma$ and $x_\ell = [\ell(\ell+1)]^{-1/4}$ denotes the location of the inner limit of the rotational barrier, i.e., it is the value of $x_b = R_b/\sigma$ in table 2 for the considered ℓ . At this point the centrifugal and van der Waals interactions exactly balance each other out. The amplitude of the s -wave ($\ell = 0$) radial wave function, $y_{\ell=0}^{I=0}(x)$, is never resonant and thus always rather small in this x -range. Close to threshold, the van der Waals interaction prevails. Treating the rotational kinetic energy as a first order perturbation introduces a resonant correction proportional to $\ell(\ell+1)$ in the ℓ -wave radial wavefunction of the field-free molecule. At intermediate distance $y_{\ell>0}^{I=0}(x) \approx y_{\ell=0}^{I=0}(x) + \ell(\ell+1)z(x)$. When evaluating the integral in equation (8), the zeroth order contribution is small, and in the first order, only the cross term $y_{\ell=0}^{I=0}(x)x^{-3}z(x)$ contributes significantly. As the energy varies, resonant behavior might appear, with a maximum of the radial

Table 3. Position and width of the $^{88}\text{Sr}_2$ field-free shape resonances with $\ell = 4, 8, 12$ and 16 , both in reduced and SI units, as calculated in [14] in a multi-channel asymptotic model with the nodal line technique.

	$\ell = 4$	$\ell = 8$	$\ell = 12$	$\ell = 16$
Position (red. units)	33.26	139.3	247.2	253.5
Position (mK)	2.872	12.03	21.35	21.89
Width (red. units)	11.48	0.9159	2.141×10^{-3}	8.778×10^{-12}
Width (μK)	991.3	79.11	0.018 49	7.582×10^{-10}

integral and therefore an energy shift with respect to the field-shifted dissociation limit approximately proportional to $\mathcal{I} \alpha(\ell) \ell(\ell + 1)$, i.e., proportional to $\mathcal{I} \ell(\ell + 1)$.

For non-zero non-resonant light, this result remains valid only as long as the interaction with the light can be considered as a perturbation compared to the centrifugal interaction, i.e., for $\mathcal{I} \ll 6 \ell(\ell + 1)x_{0\ell}$, in the x -domain mainly contributing to the integral, i.e., for $x_{0\ell} < x < x_\ell$. Therefore, for a given intensity \mathcal{I} , the deviation of the reduced energy shift from the approximate universal law is larger for smaller ℓ -values.

The observation of an approximately universal intensity-dependence of the reduced energy shifts can be equivalently formulated as follows: In order to shift the position of two shape resonances with field-free rotational quantum numbers ℓ_1 and ℓ_2 in two molecules, 1 and 2, by the same amount, the reduced laser intensities \mathcal{I}_1 and \mathcal{I}_2 must be related as

$$\mathcal{I}_1 \ell_1(\ell_1 + 1) \approx \mathcal{I}_2 \ell_2(\ell_2 + 1). \quad (10)$$

We emphasize that this rule provides only the approximate *slope* of the energy variation at $\mathcal{I} \rightarrow 0$. To obtain the energy variation itself, one also has to know the field-free reduced energy of the shape resonance, i.e., the s -wave scattering length [13, 21].

4. Slopes at vanishing intensity from perturbation theory

Since the intensity dependence of the shape resonance positions appears to be linear up to large values of the field intensity, it is interesting to study the behavior at very low intensity and calculate the slopes at $\mathcal{I} = 0$. This procedure requires only free-field calculations, that is a single-channel model. In principle, the perturbation theory has here to be applied to a continuous spectrum. We discuss the example of the $^{88}\text{Sr}_2$ shape resonances with field-free $\ell = 4, 8, 12, 16$, whose positions and widths are recalled in table 3. We present results obtained by the single-channel nodal line technique, with a detailed description of the resonance profiles, and compare them to those obtained by solving the Schrödinger equation with Hamiltonian (1), using a discretization of the scattering continuum.

4.1. Single-channel nodal line technique

The description of the perturbation of a shape resonance by a weak interaction takes a rather simple form in the nodal line formalism. It is described in appendix, with no particular shape of the potentials involved in the zero and first order expressions. In the case of interest here, the unperturbed asymptotic Schrödinger equation for the radial wave function of wave ℓ reads, in reduced units,

$$\left[-\frac{d^2}{dx^2} - \frac{1}{x^6} + \frac{\ell(\ell + 1)}{x^2} - \mathcal{E} \right] y^{(0)}(x) = 0, \quad (11)$$

where we have omitted, compared to equation (5), the index ℓ of the radial function $y(x)$ for simplicity. The superscript denotes the order of perturbation theory. The perturbation is given by

$$h_{\text{int}} = \mathcal{I}v(x) = -\mathcal{I} \frac{\alpha(\ell)}{x^3}. \quad (12)$$

Let us recall that in the nodal line formalism (see section III B of paper I [14]), equation (11) is only solved in the asymptotic x domain, $x > x_0$ (here also the index ℓ is omitted for simplicity). The interactions in the inner zone (potential, rotational kinetic energy) in the zeroth order Hamiltonian are accounted for by the choice of the node position, equation (6). In the perturbative treatment of the interaction with the non-resonant field, contributions to first order coming from the inner zone have thus to be accounted for separately.

In a first step, we ignore the variation of the node position to treat the problem in the outer zone. The reduced slopes of position and width of the resonance can be obtained by calculating the perturbation of the energy profile of the phaseshift characterizing the resonance structure (see appendix A 2 of paper I [14]). This perturbation, written in the Born approximation [22], cf equation (A.8), is equal to $\frac{d}{d\mathcal{I}} \Delta \delta_{\text{out}}(\mathcal{E}) = -\pi \mathcal{J}_{\text{out}}(\mathcal{E})$

Table 4. Reduced slopes (i.e., slopes in reduced units, divided by $\ell(\ell + 1)$) of the resonance position's intensity dependence for $^{88}\text{Sr}_2$ and $\ell = 4, 8, 12$ and 16 from different approaches. The first four lines are obtained with the single-channel perturbative approach described in appendix: lines 1 and 3: including only the asymptotic outer part of the perturbation, equation (13). Lines 2 and 4: taking also the inner part through the intensity-dependence of the node position, equation (14), into account. The first two lines are obtained by fitting the derivative of the phase shift with respect to \mathcal{I} to equation (A.6). The following two lines (marked by a star) correspond to the simplified formula, equation (A.9), which ignores the intensity dependence of the width. The fifth line results from a calculation similar to those reported in paper I [14], i.e., using an asymptotic single-channel model with \mathcal{I} -dependent nodal lines. The last line lists the slopes of the node position's intensity-dependence used in paper I [14]; they are required to obtain the reduced slopes in lines 2 and 4.

	$\ell = 4$	$\ell = 8$	$\ell = 12$	$\ell = 16$
Outer	-0.0791	-0.0710	-0.0602	—
Outer+inner	-0.0931	-0.101	-0.100	—
Outer*	-0.114	-0.0713	-0.0602	-0.0521
Outer+inner*	-0.137	-0.101	-0.100	-0.102
Calc cf I	-0.0941	-0.101	-0.100	-0.0954
$dx_0/d\mathcal{I}$	4.417×10^{-5}	4.525×10^{-5}	4.873×10^{-5}	5.497×10^{-5}

Table 5. Same as table 4 but for the width instead of the position of the resonances (lines 3 and 4 are omitted since the simplified formula, equation (A.9), does not give any information on the intensity dependence of the width). The resonance with $\ell = 16$ is so extremely narrow that the intensity-dependence of its width cannot be obtained.

	$\ell = 4$	$\ell = 8$	$\ell = 12$	$\ell = 16$
Outer	-1.44	-0.213	-0.000 089 1	—
Outer + inner	-1.88	-0.324	-0.000 156	—
Calc cf I	-1.69	-0.329	-0.000 160	—

with

$$\begin{aligned} \mathcal{J}_{\text{out}}(\mathcal{E}) &= -\frac{1}{\pi} \frac{d}{d\mathcal{I}} \Delta\delta_{\text{out}}(\mathcal{E}) \\ &= -\alpha(\ell) \int_{x_0}^{\infty} \frac{1}{x^3} [y^{(0)}(x)]^2 dx, \end{aligned} \quad (13)$$

where $F_0(x) = y^{(0)}(x)$ is the field-free energy-normalized physical regular radial function ($F_0(x_0) = 0$). Assuming a Lorentzian shape of the derivative of the phaseshift with respect to energy, one obtains for this derivative in equation (13) the right-hand side of equation (A.6). A simple fit procedure thus yields the slopes at $\mathcal{I} = 0$ of both position and width of the resonance (cf first line of tables 4 and 5), except for the extremely narrow resonance with $\ell = 16$, for which the slopes cannot be obtained. The simplified formula of equation (A.9) gives roughly the same result for the slope of the position as the fitting procedure (compare first and third lines of table 4), except for the broadest resonance ($\ell = 4$).

The nodal line formalism allows us to also account for the modifications due to the internal part of the non-resonant field perturbation which changes the node position x_0 . One can calculate the displacement of the node positions with the complete Hamiltonian (see paper I [14]): for instance, the slopes $\frac{dx_0}{d\mathcal{I}}$ of the intensity dependence of the node positions at $\mathcal{I} = 0$ are listed in the last line of table 4 for $\ell = 4, 8, 12, 16$ in $^{88}\text{Sr}_2$. If no reliable data are available for the full potential, it is possible to use a 'universal' value for these slopes (see equation (19) below). We show in the appendix that a simple relationship, equation (A.12), exists between the intensity dependence of the node position and the corresponding modification of the slope of the intensity dependence of the phaseshift $\frac{d}{d\mathcal{I}} \Delta\delta_{\text{in}}(\mathcal{E}) = -\pi \mathcal{J}_{\text{in}}(\mathcal{E})$, corresponding to the contribution of the inner zone, with

$$\mathcal{J}_{\text{in}}(\mathcal{E}) = -\frac{1}{\pi} \frac{d}{d\mathcal{I}} \Delta\delta_{\text{in}}(\mathcal{E}) = \frac{dx_0}{d\mathcal{I}} \frac{1}{\pi^2 G_0(x_0)^2}. \quad (14)$$

Here $G_0(x_0)$ is the value at x_0 of the energy-normalized irregular solution of the Schrödinger equation, which is orthogonal to the physical regular one, $F_0(x) = y^{(0)}(x)$, which has a node at x_0 . Adding this quantity to the one coming from equation (13) and repeating the above fitting procedure for the sum yields the total slopes of both position and width of the resonance (see the second line in table 4 and table 5). The agreement with the slopes calculated with the full potential is excellent (compare lines 2, 4 and 5 of table 4, and lines 2 and 3 of table 5).

Table 6. Reduced slopes (i.e., slopes in reduced units, divided by $\ell(\ell + 1)$) of the resonance position's intensity dependence for $^{88}\text{Sr}_2$ and two different sizes R_{max} of the discretization box, computed with Hamiltonian (1) and a DVR (lines 1 and 2) compared to perturbation theory (PT) using the full potential (lines 3 to 6). PT can employ additionally the asymptotic approximation for the interaction term, equation (16) (lines 3 and 4), or treat the full interaction with the non-resonant light, equation (15) (lines 5 and 6). For the narrow resonances $\ell = 12$ and 16 , the reduced slopes are evaluated from a single L^2 -normalized wave function, whereas for the broad resonances, an integration over the Lorentzian resonance profile is carried out (see text for details). These reduced slopes are to be compared to those reported in table 4.

	$R_{\text{max}} (a_0)$	$\ell = 4$	$\ell = 8$	$\ell = 12$	$\ell = 16$
Non-PT	1×10^5	-0.1026	-0.1029	-0.1013	-0.0952
Non-PT	2×10^5	-0.1010	-0.1030	-0.1017	-0.0952
PT $\langle x^{-3} \rangle$	1×10^5	-0.107	-0.0856	-0.0900	-0.0827
PT $\langle x^{-3} \rangle$	2×10^5	-0.105	-0.0854	-0.0904	-0.0827
Full PT	1×10^5	-0.111	-0.0933	-0.1011	-0.0952
Full PT	2×10^5	-0.109	-0.0931	-0.1017	-0.0952

4.2. Full potential calculations and discretized continuum

Our calculations of the resonance positions with the full potential employ a DVR [16]. This implies that the continuum spectrum is discretized in a finite box of size R_{max} and represented by means of L^2 -normalized wave functions with energies $E_n > 0$. Energy-normalized discretized continuum wavefunctions are obtained by multiplication with $1/\sqrt{E_n - E_{n-1}}$. When considering the full Hamiltonian (1), a resonance for partial wave ℓ is identified in the discretized spectrum by plotting the rotational constant $\langle \hbar^2/(2\mu R^2) \rangle$ for the ℓ -component of the coupled channels wavefunction as a function of energy. Very narrow resonances, such as those with $\ell = 12$ or $\ell = 16$ in $^{88}\text{Sr}_2$, cf table 3, appear as δ -functions at the corresponding resonance energy, independent of the size of the box R_{max} . For the other two $^{88}\text{Sr}_2$ resonances considered here, with $\ell = 4$ and $\ell = 8$, the widths are broader. The resonances are thus described by more than one eigenvalue of the discretized spectrum. The resonance position is then obtained by fitting the rotational constants, computed using energy-normalized wave functions [23, 24], to a Lorentzian profile. Once resonance positions are obtained, their intensity-dependence can be fitted to a line in the weak field regime. The corresponding slopes, divided by $\ell(\ell + 1)$ are presented in table 6 (lines 1 and 2). Their weak dependence on the size of the box indicates the accuracy of our continuum discretization.

Analogously to the previous subsection, we treat the interaction with the non-resonant light, i.e., the last term in the full Hamiltonian (1), as a perturbation to the field-free Hamiltonian. This is motivated by the approximately linear dependence of the resonance positions on field intensity up to fairly large intensity. We distinguish between narrow and broad resonances. For a narrow resonance, which is associated to a single discretized energy, time-independent perturbation theory provides the following first-order correction to the resonance energy [25, 26]

$$\Delta E_{n,\ell} = -\frac{2\pi I}{c} \left[\langle \psi_{n,\ell} | \alpha_{\perp}(R) | \psi_{n,\ell} \rangle - (\alpha_1 + \alpha_2) + \langle \psi_{n,\ell} | \Delta\alpha(R) | \psi_{n,\ell} \rangle \frac{2\ell^2 + 2\ell - 1}{(2\ell + 3)(2\ell - 1)} \right], \quad (15)$$

where $\psi_{n,\ell}$ is the field-free L^2 -normalized wave function of the resonance. When using additionally the asymptotic approximation for the interaction Hamiltonian at sufficiently large distance, equation (2), the first-order correction to the energy shift with respect to the field-dressed dissociation limit, $E_0 = -2\pi I(\alpha_1 + \alpha_2)/c$, becomes (in reduced units)

$$\Delta \mathcal{E}_{n\ell} = -I \langle \psi_{n,\ell} | x^{-3} | \psi_{n,\ell} \rangle \alpha(\ell), \quad (16)$$

where $\alpha(\ell)$ is given in equation (9). Equation (16) is equivalent to equation (8). Equations (15) and (16) provide an approximation to the slopes of the intensity dependence of the resonance positions, valid within the limits of a weak perturbation and for a narrow resonance.

For broad resonances, equations (15) and (16) can also be used. However, the complete profile of the matrix element of the perturbation needs to be evaluated. To this end, energy-normalized wave functions have to be considered. In our example of $^{88}\text{Sr}_2$, the resonance profiles are made up by about 40 energies for $\ell = 4$ and 5 for $\ell = 8$. We decompose the energy dependence of the matrix elements into a Lorentzian plus a slowly varying background. This is important in particular for the resonance $\ell = 4$, which is very broad such that it extends

down to the threshold (see table 3). The final mean value of the perturbation is determined by integrating the matrix elements, equations (15) and (16), over the Lorentzian.

For both broad and narrow resonances, the values obtained with perturbation theory are reported in table 6 for two different sizes of the discretization box, where equation (16) was employed in lines 3 and 4 and equation (15) in lines 5 and 6, together with the results from multi-channel calculations with the full Hamiltonian (1) (lines 1 and 2). The results are converged with respect to the continuum discretization since the differences between the two sizes of the box are very small, below 2%, for all ℓ values and all treatments. For the non-perturbative multi-channel calculations, the excellent agreement between the asymptotic model (with the reduced slopes reported in line 5 of table 4) and the full Hamiltonian (lines 1 and 2 of table 6) found in [14] is confirmed: the values differ by less than 2%, except for $\ell = 4$, where the difference is of the order of 10%. This observation for $\ell = 4$ is most likely due to the different choice of profile used in the analysis—the lowest eigenvalue of the delay matrix in the nodal line method as opposed to the rotational constant, i.e., the mean value of R^{-2} , in the full potential calculations. For broad resonances these two profiles are known to be rather different [13]. The otherwise good agreement allows to assess the accuracy of the perturbation theory treatment, in particular in form of the single-channel nodal line technique, when using intensity-dependent nodal lines.

For the narrow resonances, with $\ell = 12$ and $\ell = 16$, the reduced slopes obtained within perturbation theory using the full interaction with the non-resonant light, cf equation (15) and lines 5 and 6 of table 6, are very close to the multi-channel calculations (lines 1 and 2 of table 6), deviating by at most 2%. A somewhat larger deviation, of about 10%, is observed for the reduced slopes obtained when neglecting the R^{-6} contribution to the polarizability anisotropy at short range, cf equation (16) and lines 3 and 4 of table 6. A similar difference between the two perturbation theory treatments is also observed for $\ell = 4$ and $\ell = 8$. A small deviation from the asymptotic model for the interaction with the non-resonant field thus persists at short range. The agreement between the multi-channel calculations (lines 1 and 2 of table 6) and the single-channel perturbation theory treatment accounting for the full interaction with the non-resonant light, using equation (15) and referred to as 'full PT' in lines 5 and 6 of table 6, for $\ell = 4$ and $\ell = 8$ is slightly worse than for the narrow resonances, with a difference of about 10%. The values obtained from nodal line technique, both perturbative (line 2 of table 4) and non-perturbative (line 5 of table 4) are closer to the multi-channel results for $\ell = 8$, but for $\ell = 4$ the difference also amounts to about 10%. For $\ell = 8, 12$ and 16 , the perturbative nodal line technique yields the most accurate values when contributions from the inner part are accounted for in addition to the x^{-3} approximation of equation (12). It is due to the fact that the intensity-dependence of the nodal lines is evaluated using this complete formula, cf equation (14).

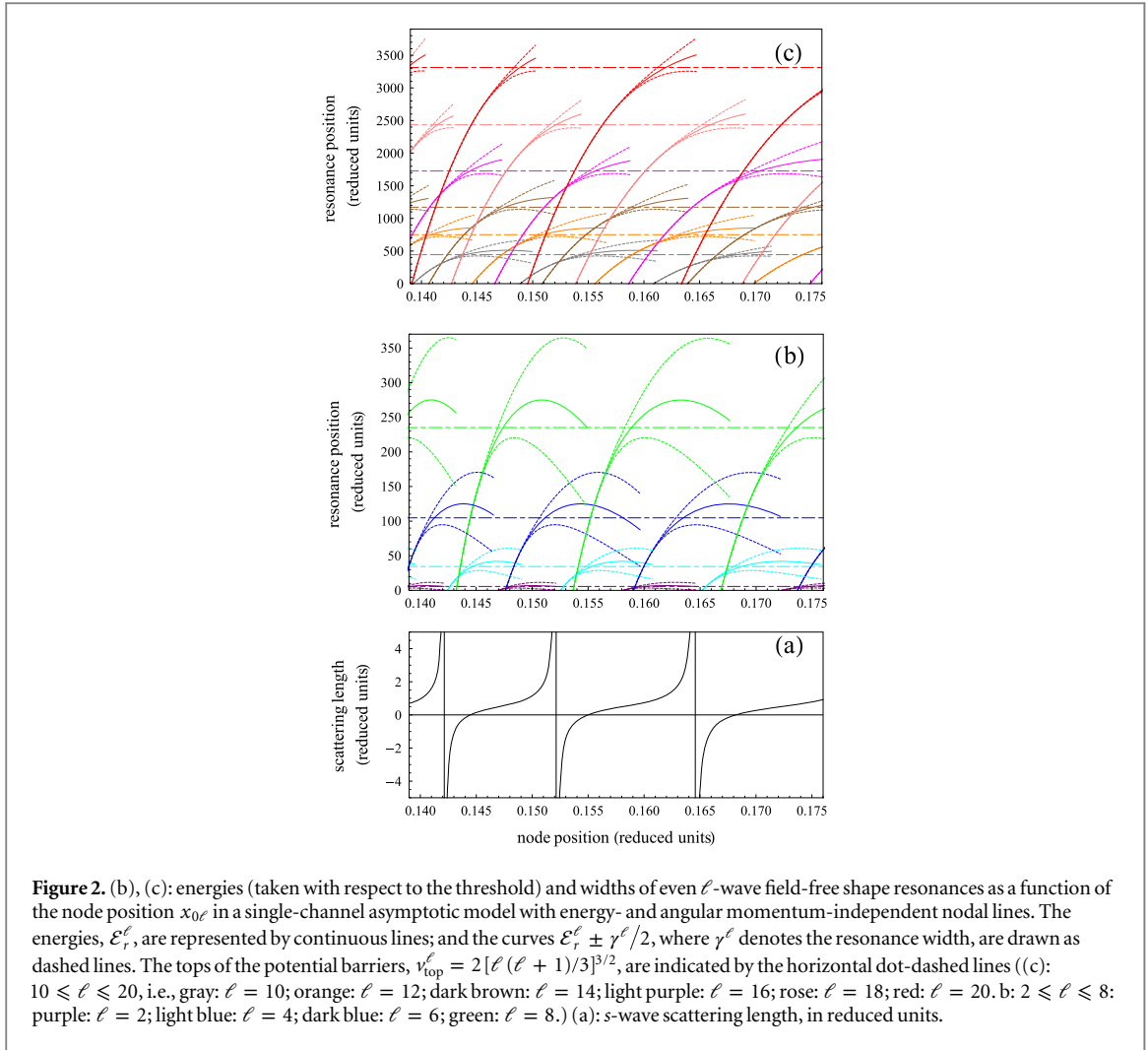
To summarize, all values obtained for the reduced slopes within perturbation theory in tables 4 and 6 are close to the non-perturbative ones and very similar for the two methods. In other words, the perturbative single-channel approximation works very well, both in the nodal line technique, provided intensity-dependent nodal lines are considered, and in the full potential calculations with a discretized continuum, provided an integration over the resonance profile is carried out for broad resonances which do not reduce to a δ -function. Moreover, and importantly so, the perturbative values of the ' ℓ -reduced' slopes are the same for different ℓ . The perturbation theory treatment thus confirms our heuristic scaling rule, equation (10).

5. Systematic single-channel calculations: general trends

The good agreement between perturbation theory and full potential calculations shown in the previous section indicates that a single-channel approximation may be sufficient for many purposes. Specifically, we use the single-channel approximation in section 5.1 to predict the position and width of shape resonances (without any non-resonant field). This extends the approach of [13], simplifying the required calculations. Second, in section 5.2, we employ the single-channel approximation to investigate universality of the intensity-dependence of shape resonances exposed to non-resonant light.

5.1. Field-free case

In the single-channel asymptotic model using the nodal line technique, the only parameter relevant for the partial wave ℓ is the node position, $x_{0\ell}$, which determines the position and width of shape resonances. The characteristics of the resonances can be determined using the complex energy method, described in section A 3 of paper I [14], for narrow resonances, or employing the energy profile of the phase shift, see section A 2 in paper I [14], for broad resonances close to the top of the potential barrier. The resonance position as a function of node position is shown in figure 2 for even ℓ ranging from 2 to 20 and for node positions $0.139 \leq x_{0\ell} \leq 0.176$. In figure 2, a single abscissa is used for the various $x_{0\ell}$, which is as if the dependence of the nodal lines on energy and angular momentum had been neglected, i.e., it is equivalent to $x_{00} = x_{0\ell}$, or $A = B = 0$ in equation (6). The resonance position shows a pseudo-periodic dependence on node position: for



each ℓ value, separate branches appear successively, with discontinuities occurring at ℓ -dependent values $x_{0\ell}$ such that $J_{(2\ell+1)/4}(1/(2x_{0\ell}^2)) = 0$, where J_ν denotes a regular Bessel function. When this condition is fulfilled, a bound level with angular momentum ℓ reaches the threshold and becomes a shape resonance. Correspondingly, the number of bound ℓ -levels is decreased by one, as is the number of nodes of the resonance wave function inside the potential barrier, $x_{0\ell} < x < x_\ell$. Between two consecutive discontinuities, along a given branch, the resonance energy increases from threshold, reaches the top of the potential barrier, $v_{\text{top}}^\ell = 2[\ell(\ell+1)/3]^{3/2}$, and even passes over the top of the barrier, with the resonance profile becoming very broad. The dependence of the reduced s -wave scattering length on x_{00} (see equation (12) of [13]) is also shown in figure 2. It exhibits an analogous pseudo-periodic pattern, and the presence of an $\ell = 0$ bound level just at threshold corresponds, as is well known, to infinite scattering length. One can see in figure 2 that, for a given value of the scattering length, there is never more than one resonance below the top of a particular ℓ -potential barrier; and when a resonance appears in a particular ℓ -channel, resonances also appear in the $\ell \pm 4p$ (p integer) channels. In order to properly account for the contribution of the potential and centrifugal term at short range, $x < x_{00}$, the nodal lines need to depend on both energy and angular momentum [13]. The results presented in figure 2 can easily be extended to energy- and angular momentum-dependent node positions $x_{0\ell}$: the dependence on angular momentum simply introduces ℓ -dependent translations parallel to the horizontal axis. The energy-dependence modifies the shape of the curves shown in figure 2 only slightly. The position and width of field-free resonances of any molecule can be estimated from figure 2, once the nodal lines $x_{0\ell}$, equation (6) have been chosen (we use in this section the 'universal' asymptotic model [13], with $A = A^G = -(x_{00})^7/8$, $B = B^G = (x_{00})^5/4$ and $C = 0$, resulting in nodal lines depending only on x_{00}). The results of the transformation $\mathcal{E}_r(x_{0\ell}) \rightarrow \mathcal{E}_r(x_{00})$ are presented in figure 3, with the abscissa now being actually x_{00} . In addition, for the figure to be more compact, we have divided \mathcal{E}_r^ℓ by the height of the corresponding rotational barrier v_{top}^ℓ . Figure 3 is useful to predict, at least roughly, the position of shape resonances of a molecule with s -wave scattering length a_S : the resonances lie on the vertical line located at the abscissa $a(x_{00}) = a_S$ (with a_S in reduced units). The dashed vertical lines in figure 3

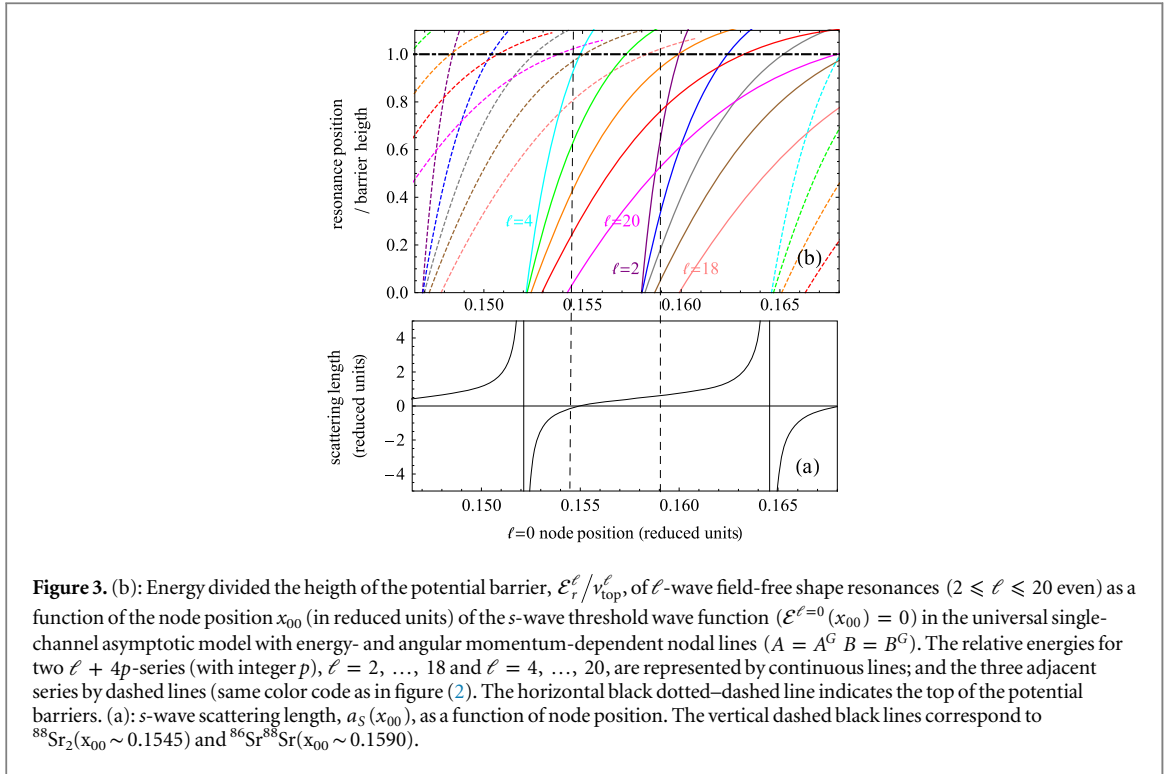


Figure 3. (b): Energy divided the height of the potential barrier, $\mathcal{E}_r^\ell/v_{\text{top}}^\ell$, of ℓ -wave field-free shape resonances ($2 \leq \ell \leq 20$ even) as a function of the node position x_{00} (in reduced units) of the s -wave threshold wave function ($\mathcal{E}^{\ell=0}(x_{00}) = 0$) in the universal single-channel asymptotic model with energy- and angular momentum-dependent nodal lines ($A = A^G B = B^G$). The relative energies for two $\ell + 4p$ -series (with integer p), $\ell = 2, \dots, 18$ and $\ell = 4, \dots, 20$, are represented by continuous lines; and the three adjacent series by dashed lines (same color code as in figure (2)). The horizontal black dotted-dashed line indicates the top of the potential barriers. (a): s -wave scattering length, $a_s(x_{00})$, as a function of node position. The vertical dashed black lines correspond to $^{88}\text{Sr}_2(x_{00} \sim 0.1545)$ and $^{86}\text{Sr},^{88}\text{Sr}(x_{00} \sim 0.1590)$.

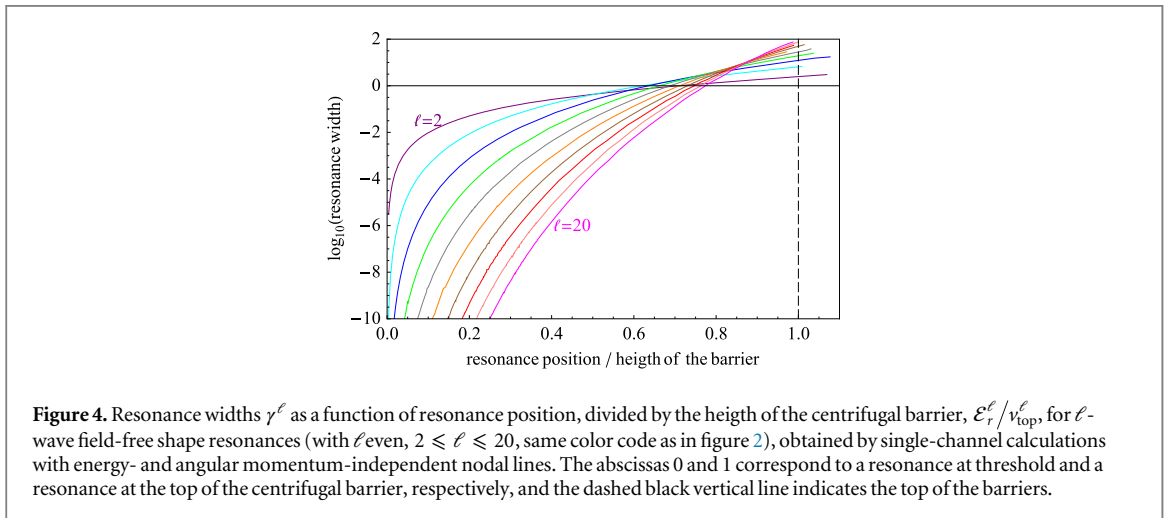


Figure 4. Resonance widths γ^ℓ as a function of resonance position, divided by the height of the centrifugal barrier, $\mathcal{E}_r^\ell/v_{\text{top}}^\ell$, for ℓ -wave field-free shape resonances (with ℓ even, $2 \leq \ell \leq 20$, same color code as in figure 2), obtained by single-channel calculations with energy- and angular momentum-independent nodal lines. The abscissas 0 and 1 correspond to a resonance at threshold and a resonance at the top of the centrifugal barrier, respectively, and the dashed black vertical line indicates the top of the barriers.

indicate the examples of $^{88}\text{Sr}_2$ and $^{86}\text{Sr},^{88}\text{Sr}$ studied in paper I, with the scattering lengths equal to $a_s = -2 a_0$ [27] or -0.013 reduced units and $a_s = 97.9 a_0$ [28] or 0.664 reduced units, respectively. Note that, for a given molecule, the resonance energies relative to the barrier tops, $\mathcal{E}_r^\ell/v_{\text{top}}^\ell$, generally decrease regularly with increasing ℓ . Note also that shape resonances with $\ell = 4p$ (p integer, not too high) appear at threshold for a reduced scattering length with large absolute value, whereas shape resonances with $\ell = 4p + 2$ appear at threshold for a reduced scattering length close to 0.48 . This property had been derived analytically by Gao [29] by solving the Schrödinger equation for a x^{-6} potential plus centrifugal term limited at $x_0^G \rightarrow 0$ by an infinite repulsive wall [29, 30]. With this potential, analytical values for the reduced s -wave scattering length a_s^G and the wall position x_0^G for which the last, least-bound rotational levels $\ell = 1, 2, 3, 4$ modulo 4 are located exactly at the dissociation limit, have been obtained [29, 30]. For $x_{00} \rightarrow 0$, the 'universal' asymptotic nodal line model becomes equivalent to Gao's universal model.

For completeness, figure 4 presents the widths of the field-free resonances, calculated in the single-channel asymptotic model, as a function of resonance energy. These widths are already visible in figure 2, where they are represented by the distance between the dotted lines around each resonance. Figure 4 shows the general trend of the widths as a function of the energy relative to the top of the barrier: At threshold, the resonances have a vanishing width, which rapidly increases when the resonance energy increases (note the logarithmic scale). At

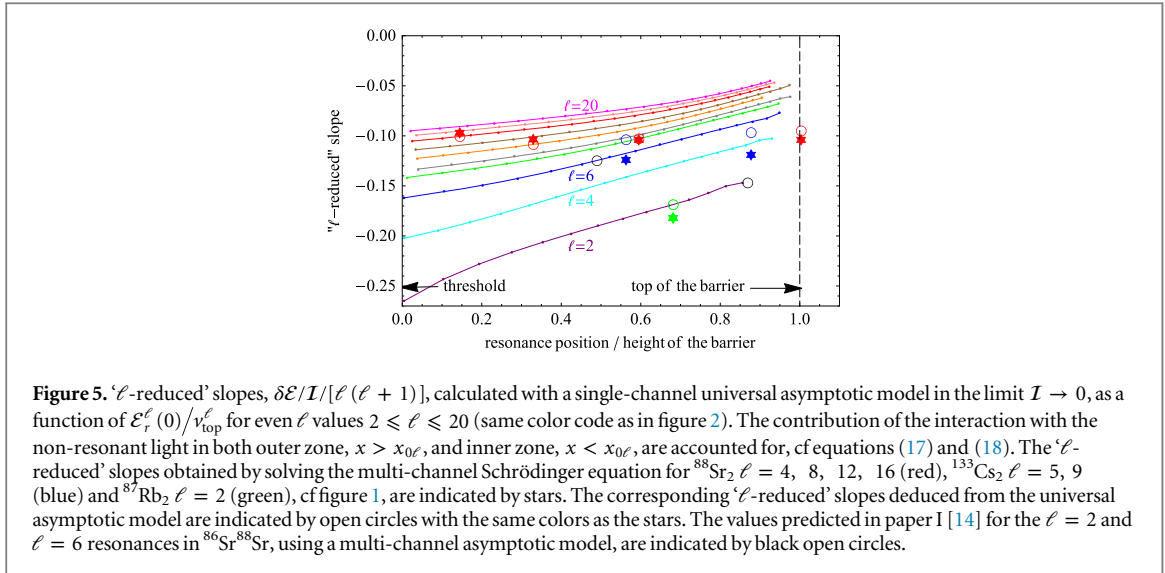


Figure 5. ‘ ℓ -reduced’ slopes, $\delta\mathcal{E}/\mathcal{I}/[\ell(\ell+1)]$, calculated with a single-channel universal asymptotic model in the limit $\mathcal{I} \rightarrow 0$, as a function of $\mathcal{E}_r^\ell(0)/v_{\text{top}}^\ell$ for even ℓ values $2 \leq \ell \leq 20$ (same color code as in figure 2). The contribution of the interaction with the non-resonant light in both outer zone, $x > x_{0\ell}$, and inner zone, $x < x_{0\ell}$, are accounted for, cf equations (17) and (18). The ‘ ℓ -reduced’ slopes obtained by solving the multi-channel Schrödinger equation for $^{88}\text{Sr}_2$ $\ell = 4, 8, 12, 16$ (red), $^{133}\text{Cs}_2$ $\ell = 5, 9$ (blue) and $^{87}\text{Rb}_2$ $\ell = 2$ (green), cf figure 1, are indicated by stars. The corresponding ‘ ℓ -reduced’ slopes deduced from the universal asymptotic model are indicated by open circles with the same colors as the stars. The values predicted in paper I [14] for the $\ell = 2$ and $\ell = 6$ resonances in ^{86}Sr - ^{88}Sr , using a multi-channel asymptotic model, are indicated by black open circles.

the top of the potential barrier, the resonance width is rather huge, between 1 and 100 reduced units. This general behavior is observed for all partial waves.

5.2. Universality in the non-resonant light control of shape resonances at low intensity

The linearity of the intensity dependence of the resonance positions observed in paper I [14] and the validity of perturbation theory at low intensity suggest a more detailed investigation of the field-dressed resonances in the universal asymptotic model. To this aim, we determine the position of the field-dressed resonances, $\mathcal{E}_r^\ell(\mathcal{I})$, at very small field intensity ($\mathcal{I} = 0.01$ reduced units) as a function of node position $x_{0\ell}$, in the range $0.139 \leq x_{0\ell} \leq 0.176$, and for partial waves with even ℓ -value, with $2 \leq \ell \leq 20$. For the same partial wave and the same $x_{0\ell}$ value, the resonance position without non-resonant field is denoted by $\mathcal{E}_r^\ell(0)$. When determining these two resonance positions, the contribution of the non-resonant field is accounted for only in the ‘outer’ zone, $x > x_{0\ell}$. The contribution of the field to the ‘ ℓ -reduced’ slope of the resonance position’s intensity-dependence in the outer zone can therefore be quantified as

$$S_{\text{out}} = \frac{\mathcal{E}_r^\ell(\mathcal{I}) - \mathcal{E}_r^\ell(0)}{\mathcal{I}\ell(\ell+1)}. \quad (17)$$

The contribution of the non-resonant field in the ‘inner’ zone results, as described in I [14], in a change of the node position proportional to the field intensity. With equation (6), this change becomes $dx_{0\ell}/d\mathcal{I} = C$. The contribution of the field to the ‘ ℓ -reduced’ slope in the inner zone becomes

$$S_{\text{in}} = \frac{1}{\ell(\ell+1)} \frac{d\mathcal{E}_r^\ell(0)}{dx_{0\ell}} \frac{dx_{0\ell}}{d\mathcal{I}}, \quad (18)$$

where the first derivative is evaluated from the dependence of $\mathcal{E}_r^\ell(0)$ on $x_{0\ell}$, reported in figure 2. The second derivative is taken to be equal to the value of C , $C = C^G$, in the universal asymptotic model (cf equation (13) in paper I [14]),

$$C^G = -x_{00}^4/12 + 3x_C^4/48. \quad (19)$$

Here, $x_C = R_C/\sigma$ is the position, in reduced units, at which the asymptotic expansion for the polarizabilities is truncated (see section 2 of paper I [14]). In the universal model, the total reduced slope is equal to $S = S_{\text{in}} + S_{\text{out}}$ and depends for each ℓ -value on the resonance position, $\mathcal{E}_r^\ell(0)$. Calculating $S(\mathcal{E}_r^\ell(0))$ for the same energy $\mathcal{E}_r^\ell(0)$ but using different branches for the node $x_{0\ell}$ (see figure 2) results in almost the same value. This proves the adequacy of our treatment of the different interactions (potential, rotational energy, laser field interaction) in the inner zone. Figure 5 presents the total ‘ ℓ -reduced’ slopes S as a function of the field-free resonance position relative to the height of the potential barrier, $\mathcal{E}_r^\ell(0)/v_{\text{top}}^\ell$. Although a large number of ℓ values and, in principle, any value of the scattering length is included in the calculations, strikingly, the slopes in figure 5 are contained in a rather small interval. The largest deviations occur for the lowest ℓ -values, $\ell = 2$ or 4. For a fixed ℓ -value, the slope increases slightly (i.e., its absolute value decreases) with increasing resonance energy, or, equivalently, with increasing node position $x_{0\ell}$. The absolute value of the ‘ ℓ -reduced’ slope decreases with ℓ . It presents a less pronounced variation when ℓ increases. For ℓ larger than approximately 8, the ‘ ℓ -reduced’ slope is roughly independent of ℓ , with only a weak dependence on the energy relative to the barrier height,

$\mathcal{E}_r^\ell(0)/v_{\text{top}}^\ell$. The mean value of the total ‘ ℓ -reduced’ slopes is $S(\mathcal{E}_r^\ell = 0) = -0.11 \pm 0.2$ at the dissociation limit and $S(\mathcal{E}_r^\ell = v_{\text{top}}^\ell) = -0.05 \pm 0.2$ at the top of the potential barrier.

The ‘ ℓ -reduced’ slopes obtained by solving the multi-channel Schrödinger equation with Hamiltonian (1) for the $\ell = 4, 8, 12$ and 16 resonances of $^{88}\text{Sr}_2$, the $\ell = 2$ resonance of $^{87}\text{Rb}_2$ and the $\ell = 5$ and 9 resonances of $^{133}\text{Cs}_2$, reported in figure 1, are in very good agreement with the values obtained from the universal asymptotic model, even for the highest ℓ values. The universal model thus appears suitable to predict, at least approximately, the ‘ ℓ -reduced’ slope for any diatomic molecule. Moreover, we find the heuristic scaling observed in table 3 to roughly hold in reduced units and for any value of the reduced scattering length. The approximate scaling rule therefore seems to be generally applicable, for a large number of ℓ values and for any dimer.

6. Conclusions

We have applied first order perturbation theory to the asymptotic model for shape resonance control of diatomic molecules interacting with non-resonant light developed in [14]. Our work is the first to employ an asymptotic model using the nodal line technique [10] to treat the perturbation of continuum states in the framework of collision theory, i.e., the Born approximation. As in earlier studies applying this approach to shape resonances [13, 14], we find it crucial to properly account for interactions at short range.

The perturbation theory treatment has been motivated by observing a linear dependence of the resonance position on non-resonant field intensity for several molecules with different scattering lengths and shape resonances in different partial waves. Comparison with full multi-channel calculations has revealed the perturbative approach to be valid for not too low values ℓ of the partial waves. The advantage of the perturbative approach is that it results in a single-channel model which facilitates calculations significantly. Although the non-resonant field couples partial waves with ℓ and $\ell \pm 2$, we find the single-channel perturbation approximation to be valid up to comparatively high intensity. We rationalize this finding as follows: The first order perturbation correction to the resonance energy is related to the expectation value of x^{-3} (where x denotes the interatomic separation in reduced units). The main contribution to the corresponding radial integral comes from x values just before the centrifugal barrier. In this range, the amplitude of the scattering wave functions is rather small, implying weak coupling, except at energies where a resonance appears. Since, close to threshold, resonances exist simultaneously only for ℓ and $\ell \pm 4$, the resonances themselves are not strongly coupled by the non-resonant field. Therefore an overall only weak channel mixing is observed, justifying the perturbative approach.

We have analyzed the linear dependence of the resonance position on non-resonant field intensity by introducing reduced slopes, i.e., slopes divided by $\ell(\ell + 1)$. We have observed an almost identical value for the reduced slope of several shape resonances in strontium, rubidium and cesium. The approximately identical dependence of the reduced slope on energy, relative to the height of the centrifugal barrier, is reproduced by systematic calculations using the universal asymptotic model, where the field-free scattering length is the only free parameter. Our universal model is equivalent to the multi-channel quantum defect treatment of shape resonances developed by Gao [20, 21, 29]. Fixing the value of the field-free scattering length in the universal model allows for predicting the position of field-free shape resonances [13, 21]. The corresponding predictions of our perturbative approach are less accurate for lower partial waves. In contrast, the slopes of the intensity-dependence of the resonances are well predicted even for high ℓ -values.

For all partial waves except for $\ell = 2$, the reduced slopes are found to vary regularly and in a small interval from the dissociation limit, where the resonances emerge, to the top of the centrifugal barrier, where the resonances start to dissolve. This behavior is independent of the specific molecule, it depends neither on its reduced mass, nor on its C_6 coefficient, polarizability or scattering length, characteristic of the short range interaction. The stability of the reduced slope, derived here first by generalizing observations for a small number of molecules and partial waves, presents a universal trend for field-dressed shape resonances.

The perturbative treatment developed here allows for a simple and efficient approach to determine the intensity-dependence in non-resonant light control of shape resonances since it requires single-channel calculations using the field-free resonance functions only. The slopes predicted by perturbation theory are sufficient to estimate, at least approximately, the non-resonant field intensities that are required to shift a field-free resonance to a desired position. This is important for utilizing non-resonant light control in molecule formation via photoassociation [16] or Feshbach resonances [17]. In addition to tuning the position and width of shape or Feshbach resonances, non-resonant light control can also be employed to change the s -wave scattering length. This will be studied in detail elsewhere [31].

Acknowledgments

Laboratoire Aimé Cotton is ‘Unité mixte UMR 9188 du CNRS, de l’Université Paris-Sud et de l’ENS Cachan’, member of the ‘Fédération Lumière Matière’ (LUMAT, FR2764) and of the ‘Institut Francilien de Recherche sur les Atomes Froids’ (IFRAF). RGF gratefully acknowledges a Mildred Dresselhaus award from the excellence cluster ‘The Hamburg Center for Ultrafast Imaging Structure, Dynamics and Control of Matter at the Atomic Scale’ of the Deutsche Forschungsgemeinschaft and financial support by the Spanish project FIS2011-24540 (MICINN), grants P11-FQM-7276 (Junta de Andalucía), and by the Andalusian research group FQM-207.

Appendix. Perturbation of a shape resonance in the nodal line asymptotic model

The description of the perturbation of a shape resonance by a weak interaction takes a rather simple form in the nodal line formalism. For simplicity, the following derivation assumes the use of reduced units, but no particular forms for the radial potentials involved in the zero order H_0 and first order H_1 Hamiltonians.

We consider a shape resonance associated to a Hamiltonian H_0 with position \mathcal{E}_{r_0} and width γ_0 . Let us assume that the resonance is characterized by a Lorentzian profile of the derivative $\delta'_0(\mathcal{E})$ of the phaseshift with respect to energy, (see for instance equation (1.185) in [22]),

$$\delta'_0(\mathcal{E}) = \frac{\gamma_0/2}{(\mathcal{E} - \mathcal{E}_{r_0})^2 + (\gamma_0/2)^2}. \quad (\text{A.1})$$

In the nodal line asymptotic formalism, the energy-normalized radial wave function $y^{(0)}$ for any ℓ value at any value of scattering energy $\mathcal{E} = k^2$ can be obtained from two separate inward integrations in which the asymptotic behavior of the energy-normalized solution is imposed to be either $\sin(kx)/\sqrt{\pi k}$ or $\cos(kx)/\sqrt{\pi k}$, with respective solutions $f_0(x)$ and $g_0(x)$ (see section A 2 in I). The condition imposed to the physical solution $y^{(0)}$ is to vanish at the node position $x = x_0$. The corresponding phaseshift is given by

$$\tan[\delta_0(\mathcal{E})] = -\frac{f_0(x_0)}{g_0(x_0)}. \quad (\text{A.2})$$

The solution $y^{(0)}$ is identical to the regular wave function $F_0(x)$ associated to H_0 , with an asymptotic behavior $\sin(kx + \delta_0(\mathcal{E}))/\sqrt{\pi k}$ (see [13]),

$$F_0(x) = \cos[\delta_0(\mathcal{E})]f_0(x) + \sin[\delta_0(\mathcal{E})]g_0(x). \quad (\text{A.3})$$

The linearly independent solution associated to $F_0(x)$ is the irregular wave function $G_0(x)$ given by

$$G_0(x) = -\sin[\delta_0(\mathcal{E})]f_0(x) + \cos[\delta_0(\mathcal{E})]g_0(x). \quad (\text{A.4})$$

Let us add a small perturbation characterized by a Hamiltonian $H_1 = \mathcal{I} v(x)$, where the parameter \mathcal{I} characterizes the strength of the perturbation. We assume the profile of the resonance to remain Lorentzian in the presence of this small perturbation, with the new profile depending on \mathcal{I} ,

$$\delta'(\mathcal{E}) = \frac{\gamma(\mathcal{I})/2}{(\mathcal{E} - \mathcal{E}_r(\mathcal{I}))^2 + (\gamma(\mathcal{I})/2)^2}. \quad (\text{A.5})$$

Close to $\mathcal{I} = 0$, the \mathcal{I} -dependence of $\delta'(\mathcal{E})$ is related to the derivatives at $\mathcal{I} = 0$ of the \mathcal{I} -dependencies of position and width:

$$\begin{aligned} \frac{d}{d\mathcal{I}}\delta'(\mathcal{E}) &= \frac{d\mathcal{E}_r}{d\mathcal{I}} \frac{\gamma_0(\mathcal{E} - \mathcal{E}_{r_0})}{\left[(\mathcal{E} - \mathcal{E}_{r_0})^2 + (\gamma_0/2)^2\right]^2} \\ &+ \frac{d\gamma}{d\mathcal{I}} \frac{1}{2} \frac{(\mathcal{E} - \mathcal{E}_{r_0})^2 - (\gamma_0/2)^2}{\left[(\mathcal{E} - \mathcal{E}_{r_0})^2 + (\gamma_0/2)^2\right]^2}. \end{aligned} \quad (\text{A.6})$$

The \mathcal{I} -dependence of the phaseshift can be related to the Hamiltonian H_1 : for any \mathcal{E} , the additional phaseshift $\Delta\delta_{\text{out}}(\mathcal{E})$ coming from the perturbation in the outer asymptotic domain $x > x_0$ is given, to first order in \mathcal{I} , by the Born approximation (see for instance equation (4.38) in [22]):

$$\begin{aligned}\Delta\delta_{\text{out}}(\mathcal{E}) &\sim \tan \Delta\delta_{\text{out}}(\mathcal{E}) \\ &= -\mathcal{I}\pi \int_{x_0}^{\infty} v(x) \left[y^{(0)}(x) \right]^2 dx,\end{aligned}\quad (\text{A.7})$$

where x_0 is the position of the node, such that

$$\begin{aligned}\frac{d}{d\mathcal{I}}\Delta\delta_{\text{out}}(\mathcal{E}) \\ &= -\pi \int_{x_0}^{\infty} v(x) \left[y^{(0)}(x) \right]^2 dx = -\pi\mathcal{J}_{\text{out}}(\mathcal{E}).\end{aligned}\quad (\text{A.8})$$

The derivative with respect to \mathcal{E} of the last equation has to be fitted to equation (A.6), allowing us to determine the derivatives with respect to intensity at $\mathcal{I} = 0$ of position and width of the field-dressed resonance.

For narrow resonances, the \mathcal{I} -dependence of the width is weak and the corresponding term in $\frac{dy}{d\mathcal{I}}$ can be neglected compared to the other one. This implies that the integral in equation (A.8) has a Lorentzian shape, with the same center \mathcal{E}_{r0} and width γ_0 as $\delta_0'(\mathcal{E})$ (equation A.1). If we call \mathcal{J}_m the value of the integral $\mathcal{J}_{\text{out}}(\mathcal{E})$ at $\mathcal{E} = \mathcal{E}_{r0}$, we deduce the slope of the \mathcal{I} -dependence of the resonance position at $\mathcal{I} = 0$ to be

$$\frac{d}{d\mathcal{I}}\mathcal{E}_r = +\pi\mathcal{J}_m\gamma/2 = \int_{-\infty}^{\infty} \mathcal{J}_{\text{out}}(\mathcal{E}) d\mathcal{E},\quad (\text{A.9})$$

which is equal to the strength of the interaction integrated over the whole energy-profile. For an attractive potential $v(x) < 0$, the integral $\mathcal{J}(\mathcal{E})$ and therefore the slopes $\frac{d\mathcal{E}_r}{d\mathcal{I}}$ are negative and $\Delta\delta_{\text{out}}(\mathcal{E})$, equation (A.7), is positive.

The nodal line formalism also allows to account for the perturbation due to the internal part of the perturbation H_1 at $x < x_0$, which introduces a shift Δx proportional to \mathcal{I} in the node position. A simple relationship between Δx and the corresponding modification to first order in \mathcal{I} of the phaseshift $\Delta\delta_{\text{in}}(\mathcal{E})$ can be obtained from equation (A.2)

$$\frac{d}{dx_0}\Delta\delta_{\text{in}}(\mathcal{E}) = -\frac{W(g_0, f_0)}{f_0(x_0)^2 + g_0(x_0)^2},\quad (\text{A.10})$$

where $W(g_0, f_0) = g_0 f_0' - g_0' f_0$ denotes the Wronskian (here the derivatives are taken with respect to x). Employing the property $F_0(x_0) = 0$ and the relation between the pairs of functions (f_0, g_0) and (F_0, G_0) ,

$$\begin{aligned}W(g_0, f_0) &= W(G_0, F_0) = \frac{1}{\pi}, \\ f_0(x_0)^2 + g_0(x_0)^2 &= F_0(x_0)^2 + G_0(x_0)^2 = G_0(x_0)^2,\end{aligned}\quad (\text{A.11})$$

we find

$$\frac{d}{dx_0}\Delta\delta_{\text{in}}(\mathcal{E}) = -\frac{1}{\pi G_0(x_0)^2}.\quad (\text{A.12})$$

Finally, the contribution of the inner zone to the variation of the phaseshift is, for any value of energy,

$$\frac{d}{d\mathcal{I}}\Delta\delta_{\text{in}}(\mathcal{E}) = -\frac{dx_0}{d\mathcal{I}} \frac{1}{\pi G_0(x_0)^2} = -\pi\mathcal{J}_{\text{in}}(\mathcal{E}).\quad (\text{A.13})$$

For an attractive potential $v(x)$, the shift in the node position is negative (see the value of C^G in equation 19) and $\Delta\delta_{\text{in}}(\mathcal{E})$ is positive.

This additional correction to the phaseshift coming from the inner part of the perturbation also results in a shift of the resonance position. This contribution equation (A.13) is to be added to the slope due to the asymptotic part of the perturbation equation (A.8). As above the derivative with respect to \mathcal{E} of the total slope of the change in the phaseshift associated with the perturbation H_1

$$\frac{d}{d\mathcal{I}}\Delta\delta(\mathcal{E}) = \frac{d}{d\mathcal{I}}\Delta\delta_{\text{out}}(\mathcal{E}) + \frac{d}{d\mathcal{I}}\Delta\delta_{\text{in}}(\mathcal{E}) = -\pi\mathcal{J}(\mathcal{E}),\quad (\text{A.14})$$

has to be fitted to equation (A.6) to determine the slopes at $\mathcal{I} = 0$ in the variation of the energy position and width of the field-dressed resonances.

References

- [1] Seaton M J and Steenman-Clark L 1977 *J. Phys. B: At. Mol. Phys.* **10** 2639
- [2] Greene C, Fano U and Strinati G 1979 *Phys. Rev. A* **19** 1485

- [3] Mies F H 1984 *J. Chem. Phys.* **80** 2514
- [4] Mies F H and Julienne P S 1984 *J. Chem. Phys.* **80** 2526
- [5] Gao B 1998 *Phys. Rev. A* **58** 4222
- [6] Gao B 2001 *Phys. Rev. A* **64** 010701
- [7] Jachymski K, Krych M, Juliennes P and Idziaszek Z 2013 *Phys. Rev. Lett.* **110** 213202
- [8] Jachymski K, Krych M, Julienne P S and Idziaszek Z 2014 *Phys. Rev. A* **90** 042705
- [9] Crubellier A and Luc-Koenig E 2006 *J. Phys. B: At. Mol. Opt. Phys.* **39** 1417
- [10] Crubellier A, Dulieu O, Masnou-Seeuws F, Elbs M, Knöckel H and Tiemann E 1999 *Eur. Phys. J. D* **6** 211
- [11] Pasquiou B, Bismut G, Beaufils Q, Crubellier A, Maréchal E, Pedri P, Vernac L, Gorceix O and Laburthe-Tolra B 2010 *Phys. Rev. A* **81** 042716
- [12] Vanhaecke N, Lisdat C, Tjampens B, Comparat D, Crubellier A and Pillet P 2004 *Eur. Phys. J. D* **28** 351
- [13] Londoño B E, Mahecha J E, Luc-Koenig E and Crubellier A 2010 *Phys. Rev. A* **82** 012510
- [14] Crubellier A, González-Férez R, Koch C P and Luc-Koenig E 2015 *New J. Phys.* **17** 045020
- [15] Ağanoğlu R, Lemesko M, Friedrich B, González-Férez R and Koch C P 2011 arXiv:1105.0761
- [16] González-Férez R and Koch C P 2012 *Phys. Rev. A* **86** 063420
- [17] Tomza M, González-Férez R, Koch C P and Moszynski R 2014 *Phys. Rev. Lett.* **112** 113201
- [18] Tomza M, Skomorowski W, Musiał M, González-Férez R, Koch C P and Moszynski R 2013 *Mol. Phys.* **111** 1781
- [19] Heijmen T G A, Moszynski R, Wormer P E S and van der Avoird A 1996 *Mol. Phys.* **89** 81
- [20] Gao B 2003 *J. Phys. B: At. Mol. Opt. Phys.* **36** 2111
- [21] Gao B 2009 *Phys. Rev. A* **80** 012702
- [22] Friedrich H 1998 *Theoretical Atomic Physics* 2nd edn (Berlin: Springer)
- [23] Luc-Koenig E, Vatasecu M and Masnou-Seeuws F 2004 *Eur. Phys. J. D* **31** 239
- [24] González-Férez R, Weidemüller M and Schmelcher P 2007 *Phys. Rev. A* **76** 023402
- [25] Friedrich B and Herschbach D 1995 *Phys. Rev. Lett.* **74** 4623
- [26] González-Férez R and Schmelcher P 2009 *New J. Phys.* **11** 055013
- [27] Stein A, Knöckel H and Tiemann E 2010 *Eur. Phys. J. D* **57** 171
- [28] Zhang J-C, Zhu Z-L, Liu Y-F and Sun J-F 2011 *Chin. Phys. Lett.* **28** 123401
- [29] Gao B 2004 *Eur. Phys. J. D* **31** 283
- [30] Moritz J M, Eltschka C and Friedrich H 2002 *Phys. Rev. A* **63** 042102
- [31] Crubellier A, González-Férez R, Koch C P and Luc-Koenig E Controlling the scattering length with non-resonant light: predictions of an asymptotic model, in preparation